Octakis(2-benzyloxyethylsulfanyl) Copper (II) Phthalocyanine: A New Liquid Crystalline Discotic Material with Benzyl-Terminated, Thioether-Linked Side Chains

Britt A. Minch, Wei Xia, Carrie L. Donley,† Ryan M. Hernandez, Chet Carter, Michael D. Carducci, Alice Dawson, David F. O'Brien,§ and Neal R. Armstrong*

Department of Chemistry, University of Arizona, Tucson, Arizona, 85721

Received September 17, 2004. Revised Manuscript Received December 17, 2004

The synthesis and materials properties of a new liquid crystalline phthalocyanine, octakis (2-benzyloxyethylsulfanyl) copper (II) phthalocyanine, **2**, are reported. This phthalocyanine possesses eight benzyl-terminated side chains with thioether links to the Pc core, which promote greater interaction between the discotic mesogens than has been seen in previous Pcs reported from this group which had benzyl-terminated alkoxy-based side chains. The use of thioether links to these side chains promotes a red-shift in the Q-band absorbance spectrum, small decreases in first oxidation potential, increased solution aggregation constants, and significantly higher K→LC transition temperatures than seen in conventional alkoxy-based side-chain-modified Pcs. Powders and single crystals of this material were characterized by X-ray diffraction and found to represent two closely related polymorphs. Room-temperature XRD of powders of **2** showed a monoclinic unit cell: $a = 22.81(1)$ Å, $b = 9.780(5)$ Å, $c = 19.314(6)$ Å, $\alpha = 90°$, $\beta = 106.918(14)°$, $\gamma = 90°$, $V = 4472$ Å^3, two molecules per unit cell, with a helical twist of the Pcs along the *b*-axis. The packing architecture in these powders showed a transition to an oblique (distorted rectangular, Col_{rd}) phase at temperatures in the LC regime, which was reversible upon cooling. The single-crystal diffraction data showed a monoclinic unit cell: $a = 23.911$ (18) Å, $b = 5.224(3)$ Å, $c = 39.17(3)$ Å ($c \approx \sqrt{3}a$); $\alpha = 90°$, $\beta = 96.971(14)°$, $\gamma = 90°$, volume = 4903(8) Å^3, and AFM characterization of the ⟨001⟩ plane of these single crystals clearly showed evidence for layered growth in this material. Langmuir−Blodgett films of **2**, characterized by AFM, X-ray reflectivity, and X-ray diffraction, showed hexagonal close packing of parallel Pc columns in the as-deposited film, and upon annealing, showed formation of at least two different domains, with column−column spacings of ca. 21 Å and 26 Å, corresponding to the ⟨10⟩ and ⟨01⟩ faces of a 2D lattice, closely related to the unit cell found for the polycrystalline material.

Introduction

Several classes of discotic mesophase materials (phthalocyanines, triphenylenes, hexabenzocoronenes, etc.) have emerged as promising electronic materials in technologies such as organic field-effect transistors (OFETs) and organic photovoltaics (OPVs).[1−29] These disc-shaped, extended aromatic rings can be transformed from crystalline materials, in their unsubstituted forms, to liquid crystalline materials upon addition of the appropriate side chains. We have

* To whom correspondence should be addressed. E-mail: nra@u.arizona.edu.
† Present Address: Cavendish Laboratories, Cambridge University, UK.
§ Deceased.

(1) Lemaur, V.; Da Silva Filho, D. A.; Coropceanu, V.; Lehmann, M.; Geerts, Y.; Piris, J.; Debije, M. G.; Van de Craats, A. M.; Senthilkumar, K.; Siebbeles, L. D. A.; Warman, J. M.; Bredas, J. L.; Cornil, J. *J. Am. Chem. Soc.* **2004**, *126*, 3271.
(2) van de Craats, A. M.; Warman, J. M. *Adv. Mater.* **2001**, *13*, 130.
(3) Adam, D.; Schuhmacher, P.; Simmerer, J.; Haussling, L.; Siemensmeyer, K.; Etzbach, K. H.; Ringsdorf, H.; Haarer, D. *Nature* **1994**, *371*, 141−143.
(4) Piris, J.; Debije, M. G.; Stutzmann, N.; van de Craats, A. M.; Watson, M. D.; Mullen, K.; Warman, J. M. *Adv. Mater.* **2003**, *15*, 1736.
(5) van de Craats, A. M.; Stutzmann, N.; Bunk, O.; Nielsen, M. M.; Watson, M.; Mullen, K.; Chanzy, H. D.; Sirringhaus, H.; Friend, R. H. *Adv. Mater.* **2003**, *15*, 495.
(6) van de Craats, A. M.; Warman, J. M.; deHaas, M. P.; Adam, D.; Simmerer, J.; Haarer, D.; Schuhmacher, P. *Adv. Mater.* **1996**, *8*, 823.
(7) van de Craats, A.; Stutzmann, N.; Bunk, O.; Nielsen, M. M.; Watson, M.; Mullen, K.; Chanzy, H.; Sirringhaus, H.; Friend, R. H. *Adv. Mater.* **2003**, *15*, 495−499.
(8) van Nostrum, C. F. *Adv. Mater.* **1996**, *8*, 1027−1029.
(9) Tans, S. J.; Miedema, R. G.; Geerligs, L. J.; Dekker, C.; Wu, J.; Neher, D.; Wegner, G. *Nanotechnology* **2003**, *14*, 1043−1050.
(10) Petritsch, K.; Friend, R. H.; Lux, A.; Rozenberg, G. G.; Moratti, S. C.; Holmes, A. B. *Synth. Met.* **1999**, *102*, 1776−1777.
(11) Ban, K. Z.; Nishizawa, K.; Ohta, K.; Shirai, H. *J. Mater. Chem.* **2000**, *10*, 1083−1090.
(12) Ban, K.; Nishizawa, K.; Ohta, K.; van de Craats, A. M.; Warman, J. M.; Yamamoto, I.; Shirai, H. *J. Mater. Chem.* **2001**, *11*, 321−331.
(13) Gurek, A. G.; Ahsen, V.; Luneau, D.; Pecaut, J. *Inorg. Chem.* **2001**, *40*, 4793.
(14) Andre, J. J.; Bernard, M.; Piechocki, C.; Simon, J. *J. Phys. Chem.* **1986**, *90*, 1327.
(15) Wörhle, D.; Eskes, M.; Shigehara, K.; Yamada, A. *Synthesis* **1993**, 194−196.
(16) Eichhorn, H.; Wöhrle, D.; Pressner, D. *Liq. Cryst.* **1997**, *22*, 643−653.
(17) Choi, M. T. M.; Li, P. P. S.; Ng, D. K. P. *Tetrahedron* **2000**, *56*, 3881−3887.
(18) Lux, A.; Rozenberg, G. G.; Petrisch, K.; Moratti, S. C.; Holmes, A. B.; Friend, R. H. *Synth. Met.s* **1999**, *102*, 1527−1528.
(19) Piechocki, C.; Simon, J.; Skoulios, A.; Guillon, D.; Weber, P. *J. Am. Chem. Soc.* **1982**, *104*, 5245.
(20) Osburn, E. J.; Chau, L. K.; Chen, S. Y.; Collins, N.; O'Brien, D. F.; Armstrong, N. R. *Langmuir* **1996**, *12*, 4784.
(21) Smolenyak, P.; Peterson, R.; Nebesny, K.; Torker, M.; O'Brien, D. F.; Armstrong, N. R. *J. Am. Chem. Soc.* **1999**, *121*, 8628−8636.
(22) Drager, A. S.; O'Brien, D. F. *J. Org. Chem.* **2000**, *65*, 2257−2260.
(23) Osburn, E. J.; Schmidt, A.; Chau, L. K.; Chen, S. Y.; Smolenyak, P.; O'Brien, D. F.; Armstrong, N. R. *Adv. Mater.* **1996**, *8*, 926.

10.1021/cm0483745 CCC: $30.25
Published on Web 03/05/2005

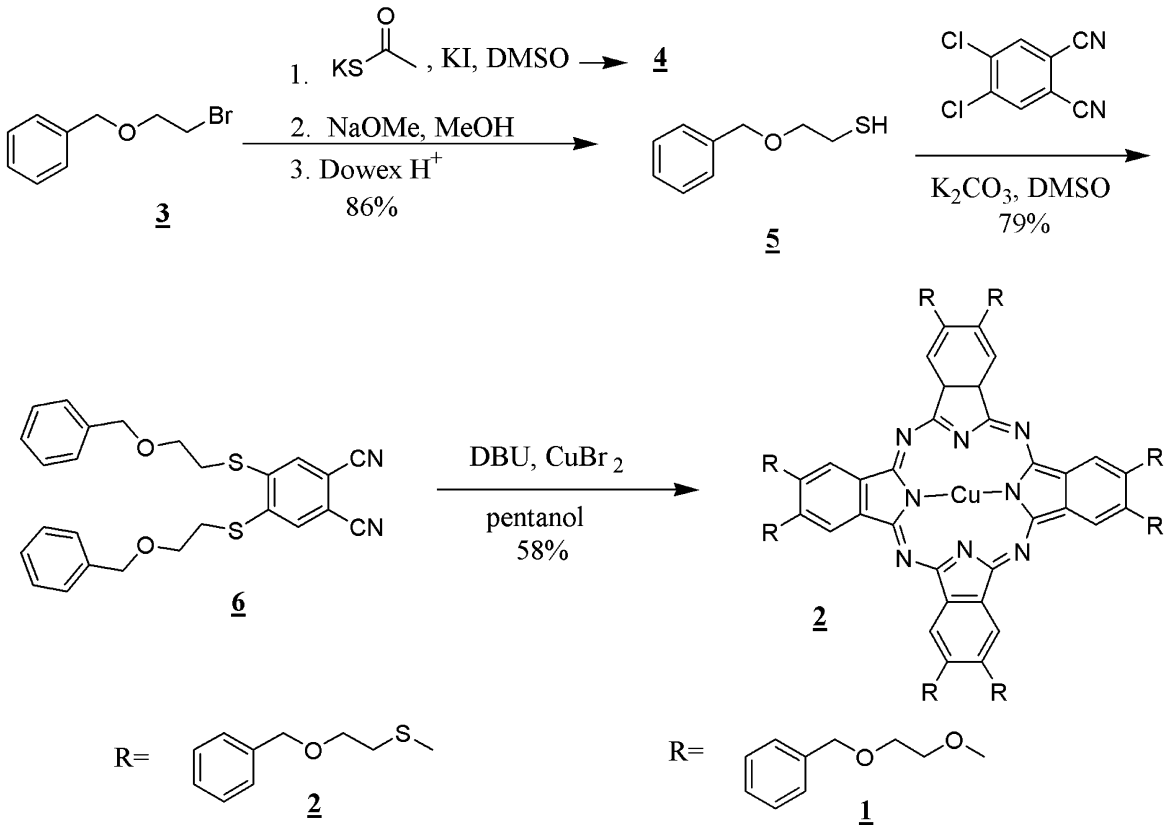

Figure 1. Schematic view of the synthetic route for Pc **2**. For synthesis of **1** see ref 19.

recently shown that octa-substituted phthalocyanines (Pcs), such as 2,3,9,10,16,17,23,24-octakis (2-benzyloxyethoxy) phthalocyaninato-copper(II) (**1**, Figure 1) self-organize into columnar aggregates, can form rigid (ca. 56−67 Å thickness) bilayers on a Langmuir−Blodgett trough, and highly coherent films on various substrates.[20−29] These alkoxy-based Pcs appear to organize themselves as would be predicted for a hexagonal discotic mesophase material—at temperatures above the crystalline-to-liquid crystalline transition (K→LC), one Pc−Pc spacing (ca. 0.35 nm) and one Pc column−Pc column spacing (ca. 2.7−2.8 nm) are seen, in X-ray diffraction data consistent with a D_h mesophase. Much of this order and spacing is retained when these materials are cooled back to room temperature. In films and fibers of these materials we have seen coherence in the rodlike aggregates of up to ca. 250 nm. Both the field effect (hole) mobilities and the dc conductivities in these films are highly anisotropic—transport along the rodlike aggregate column axis, versus perpendicular to this column axis, is favored by a factor of more than 10×, when measured on micron length scales, and 100−1000× when measured on submicron length scales.[21,25,28] The orientation of such columns is optimal for OFET applications, since it is straightforward to arrange the columns parallel to the substrate plane, with their long axis between the source and drain contacts, along the direction of preferred current flow.

A few side-chain-modified Pcs, with side chains linked to the Pc core via chalcogens (e.g., sulfur) have been reported, with apparent positive influence on the field-effect mobilities, apparently owing to the increased interaction between adjacent Pc cores due to sulfur−sulfur interactions.[10−12] Molecular materials which incorporate chalcogen atoms at critical positions appear to provide for new types of interactions in van der Waals solids. Chalcogen−chalcogen interactions between molecules are believed to be as useful as hydrogen bonding in the self-assembly of disk-shaped or ring-shaped molecules.[30] Helical LC phases have been observed in the rodlike or tube-like aggregates that form.[3] These recent studies provide the motivation for creation of generations of new phthalocyanine materials which combine the properties of our earlier Pcs, modified with benzyloxyethoxy side chains, with those obtainable from incorporation of chalcogen links to these side chains at eight peripheral positions on the Pc core.

Previous syntheses of sulfur-linked, side-chain-modified Pcs have involved high reaction temperatures and long reaction times to make alkylthiol substituted Pcs,[15,16] however, thioether linkages have been recently formed with 4,5-dichorophthalonotrile at room temperature, with short reaction times.[17,18] In this paper we focus on the synthesis and preliminary characterization of 2,3,9,10,16,17,23,34-octakis-

(24) Drager, A. S.; Zangmeister, R. A. P.; Armstrong, N. R.; O'Brien, D. F. *J. Am. Chem. Soc* **2001**, *123*, 3595−3596.
(25) Donley, C.; Xia, W.; Minch, B.; Zangmeister, R. A. P.; Drager, A. S.; Nebesny, K.; O'Brien, D. F.; Armstrong, N. R. *Langmuir* **2003**, *19*, 6512−6522.
(26) Minch, B.; Xia, W.; O'Brien, D. F.; Armstrong, N. R. manuscript in preparation.
(27) Minch, B. A. Ph.D. Dissertation, University of Arizona, 2004.
(28) Donley, C. L.; Zangmeister, R. A. P.; Xia, W.; Minch, B.; Drager, A.; Cherian, S. K.; LaRussa, L.; Kippelen, B.; Domercq, B.; Mathine, D. L.; O'Brien, D. F.; Armstrong, N. R. *J. Mater. Res.* **2004**, *19*, 2087.
(29) Xia, W.; Minch, B.; Carducci, M.; Armstrong, N. R. *Langmuir* **2004**, *20* (19), 7998−8005.
(30) Gleiter, R.; Werz, D.; Rausch, B. *Chem. Eur. J.* **2003**, *9*, 2676−2683.

(2-benzyloxyethylsulfanyl) copper(II) phthalocyanine (**2**) (Figure 1), with benzyl-terminated, thioether side chains. This Pc is the first in a series of related, sulfur-linked LC−Pcs with complex side chains.[27,31] Unlike Pc **1**, Pc **2** exhibits a highly ordered crystalline phase—powder and single crystal X-ray diffraction data suggest two closely related polymorphs, with a monoclinic unit cell and a K→Col_{rd} transition at temperatures above 134 °C, versus the K→D_h transition at ca. 63 °C seen for Pc **1**.[21,23,25,31] The Pc−Pc separation is significantly larger than 0.35 nm, considering the tilting in the disks with respect to their cofacial/upright position, and a polymorph is formed in the powder of this Pc recovered from chloroform, with a distinct helical twist of the Pc rings around the column axis. LB films of this material produce parallel columnar aggregates with good coherence, however, two different column−column spacings are observed in annealed films, which are closely related to the low index faces of the unit cell of the polycrystalline phase of this material.

Experimental Section

General Information. All nonaqueous reactions were carried out under an argon atmosphere unless stated otherwise. Reagents and solvents were purchased from Aldrich, Fluka, or TCI and were used as received unless specified otherwise. THF was distilled from Na/benzophenone. Column chromatography was performed using 300- mesh SiO_2 unless otherwise specified. The NMR spectral data for the intermediate compounds was collected using a Varian Gemini 200.

Thioacetic acid-S-(2-benzyloxyethyl) ester (4). A procedure from the literature was adapted as follows.[32] Benzyloxyethylbromide (**3**) (9.95 g, 46.0 mmol) and KI (7.64 g, 46.0 mmol) were dissolved in 35 mL of dry DMSO and the solution was degassed by bubbling argon through the solution for 10 min. The reaction was cooled to 8 °C with an ice bath, and potassium thioacetate (5.80 g, 51.0 mmol) (Aldrich) was added to the reaction mixture. The reaction was stirred overnight under argon. The reaction mixture was partitioned between 100 mL of DI water and 200 mL of ether. The aqueous solution was washed (2 × 100 mL) with ether. The combined organic layers were dried over $MgSO_4$. The solution was gravity filtered and concentrated in vacuuo to yield a yellow-tinted oil. The oil was purified by column chromatography using 80:20 hexanes/EtOAc as the eluent ($R_f = 0.93$). The weight of the purified product was 9.20 g, 95% yield. ^{1}H NMR ($CDCl_3$) δ 7.28−7.25 (m, 5H), 4.46 (s, 2H), 3.56−3.50 (t, 6.22 Hz, 2H), 3.08−3.02 (t, 6.36 Hz, 2H), 2.27 (s, 3H),. ^{13}C NMR ($CDCl_3$) δ 195.47, 137.94, 128.38, 127.64, 72.96, 68.64, 30.52, 29.01. IR (neat) 2934.48, 1687.93, 1450.00 cm^{-1}. MS analysis (ESI+) [M + H] = 211.0 (theoretical mass for $C_{11}H_{14}O_2S$ = 209.07).

Benzyloxyethanethiol (5). A procedure from ref 32 was modified as follows. Compound **4** (5.00 g, 24.0 mmol) was dissolved in 30 mL of anhydrous methanol. The solution was degassed under argon for 10 min and a degassed methanol solution (15 mL) of sodium methoxide (NaOMe) (2.30 g, 43.0 mmol) was added to the reaction mixture. The solution was stirred under argon, at room temperature, for 1 h. Dowex H^+ exchange resin, 5.00 g, was added and the reaction was stirred for an additional 30 min. The solution was gravity filtered and concentrated in vacuo to yield a yellow oil weighing 3.60 g, 90% yield. The spectral data were consistent with previous literature findings for materials of this type.[34] ^{1}H NMR ($CDCl_3$) δ 7.36−7.20 (m, 5H), 4.55 (s, 2H), 3.65−3.58 (t, 6.38 Hz, 2H), 2.77−2.67 (q, 6.38 Hz, 2H), 1.64−1.55 (t, 8.28 Hz, 1H). ^{13}C NMR ($CDCl_3$) δ 128.39, 127.66, 72.94, 71.80, 24.40. IR (neat) 3483.68, 2853.68, 2560.00, 1456.32, 688.95 cm^{-1}. MS analysis (GC/MS-basic CI) [M − H] = 167 (theoretical mass for $C_9H_{12}OS$ = 168.06).

4,5-bis-(2-Benzyloxyethylsulfanyl)phthalonitrile (6). A procedure from ref 18 was modified as follows. 4,5-Dichlorophthalonitrile (0.49 g, 2.5 mmol) and 2.6 g (20 mmol) of K_2CO_3 were suspended in 25 mL of anhydrous DMSO, which was then deoxygenated with argon. A 1.68-g (9.9 mmol) portion of **5** was added to this solution and the reaction was allowed to stir at room temperature. Using thin-layer chromatography to periodically assay this solution, the reaction appeared to go to completion at ca. 60 min. The reaction mixture was then added to a 500-mL separatory funnel and the product was partitioned between 200 mL of ether and 50 mL of water. The aqueous layer was extracted with 50 mL of ether. The combined organic layers were then washed with 50 mL of a saturated sodium chloride solution and dried over $MgSO_4$. The excess solvent was removed in vacuo. The crude product was purified by column chromatography using 70:30 hexanes/EtOAc as the eluent ($R_f = 0.78$), and the white solid was then recrystallized from methanol (79% yield, 0.91 g). ^{1}H NMR ($CDCl_3$) δ 7.55 (s, 2H), 7.36−7.32 (m, 10H), 4.55 (s, 4H), 3.79−3.73 (t, 6.22 Hz, 4H), 3.27−3.21 (t, 6.08 Hz, 4H). ^{13}C NMR ($CDCl_3$) δ 143.97, 137.97, 129.53, 128.52, 127.97, 127.64, 115.40, 111.54, 73.36, 68.07, 32.89, IR (KBr) 3071.58, 2867.89, 2578.95, 2255.16 cm^{-1}. MS analysis (FAB+) [M + H] = 461.2 (theoretical mass for $C_{26}H_{24}N_2O_2S_2$ = 460.13).

2,3,9,10,16,17,23,24-octakis(2-Benzyloxyethylsulfanyl)phthalocyanato Copper (II) (2). A literature procedure from ref 34 was adapted as follows. Compound **6** (0.369 g, 0.802 mmol) was added to a 25-mL conical flask that contained a large spin vane. Copper(II)bromide (0.047 g, 0.201 mmol) and 0.135 g (0.887 mmol) of 1,8-diazabicyclo[5.4.0]undec-7-ene (DBU) and 10 mL of 1-pentanol were next added to the flask. The reaction vessel was fitted with a reflux condenser and the reaction was brought to reflux under argon. After 24 h the reaction was allowed to cool to room temperature and was then capped and placed in the freezer for 1 h. The product was collected using vacuum filtration. The dark green solid was then washed with copious amounts of water followed by 50 mL of ether. The blue-green solid was continuously extracted with ether followed by methanol (each for 48 h) using a Soxhlet extractor. The solid was then purified by column chromatography (98:2 $CHCl_3/CH_3OH$). A dark blue-green solid was obtained (0.22 g, 58%). UV−Vis ($CHCl_3$) 712, 638, 324 nm. IR (KBr) 3445, 3048, 2920, 2851, 1099 cm^{-1}. MS analysis (MALDI) 1906.7350 (theoretical mass for $C_{104}H_{98}CuN_8O_8S_8$ = 1905.47). Elemental analysis (Desert Analytics) revealed a carbon content of ca. 65.2% (theoretical 65.3%); a hydrogen content of ca. 5.2% (theoretical 5.4%); nitrogen content of ca. 5.9% (theoretical 5.9%); and a sulfur content of ca. 12.7% (theoretical 13.4%).

The paramagnetic nature of the metal center in this type of copper phthalocyanine has been previously noted,[14] and would be expected to lead to broadening of NMR peaks. One-dimensional (1D) ^{1}H NMR spectra were acquired on a Bruker DRX-500 spectrometer at 25 °C using 128 scans, a spectral width of 26041.7 Hz, and a relaxation delay of 2.0 s. Data were processed using the Bruker software XWINNMR. Samples were dissolved in $CDCl_3$ containing

(31) Xia, W.; Carducci, M.; Armstrong, N. R. manuscript in preparation.
(32) Svedhem, S.; Hollander, C.-A.; Konradsson, P.; Shi, J.; Liedberg, B. *J. Org. Chem.* **2001**, *66*, 4494−4503.
(33) Zangmeister, R. A. P.; Smolenyak, P.; Drager, A. S.; O'Brien, D. F.; Armstrong, N. R. *Langmuir* **2001**, *17*, 7071−7078.
(34) Tomoda, H.; Saito, S.; Shiraishi, S. *Chem. Lett.* **1983**, 313−316.

0.05% (v/v) tetramethylsilane (TMS) as an internal standard. Proton chemical shifts were referenced directly to this standard at 0.00 ppm. The paramagnetic nature of the complex *did* lead to broadened peaks and significantly increased the range of chemical shifts observed. These NMR spectra are available in the Supporting Information for this paper. The effects of the paramagnetic copper center were most pronounced for protons nearest to the metal center. Thus the signals from protons on the bridging nitrogens were broadened beyond our ability to detect them. The same phenomenon led to broad peak shapes and low integral values of the peak centered around 10.38 ppm, which arises from the phenyl protons in closest proximity to the metal center. This peak is shifted significantly downfield as well, in contrast to the other set of aromatic protons found in the 7.60−7.00 ppm region. The three sets of methylene protons gave rise to three peaks observed between 5.00 and 2.50 ppm. The farthest downfield (4.55 ppm) and least broadened peak resulted from the protons adjacent to both the phenyl ring and ether oxygen. The protons on the opposite side of this ether linkage lead to the peak at 3.80 ppm. The most upfield peak, at 3.25 ppm, can be assigned to the protons nearest to the sulfur atoms. This is broadened as well, by virtue of being incrementally closer to the copper center. These results, especially the comparison of the integral values of the least broadened peaks, confirmed the identity of **2**.

Physical Characterization of Pc 2. Differential scanning calorimetry (DSC) was performed on Pcs **1** and **2** using a TA Instruments model DSC 2920/modulated DSC. A 2−3-mg portion of the powdered Pc was weighed into aluminum DSC pans and crimped shut. Pc samples were first cooled to −40 °C and heated to 250 °C at a rate of 5 °C/min. The sample was then cooled to 25 °C and finally heated to 400 °C at a rate of 10 °C/min. The DSC chamber was purged with a nitrogen flow rate of 30 mL/min during the experiment.

UV−visible spectroscopic characterization of solutions and cast or LB-deposited films of Pcs **1** and **2** were carried out with a CCD-array spectrometer (Spectral Instruments, Inc., Tucson AZ). Langmuir−Blodgett thin films of **2** were formed as described previously,[7] using a Riegler−Kirsten LB trough. Pressure−area isotherms (see below) were obtained to determine the compression needed to form either stable monolayers or bilayers of Pc **2**, and the compression needed to collapse the film into stable fibers. LB films for AFM characterization were obtained by horizontal transfer to hydrophobized Si(100) wafers. Fibers were harvested off the trough onto quartz or glass slides to provide samples for temperature-dependent polarized light microscopy (POM). POM experiments were conducted with a Nikon Eclipse ME600 outfitted with cross polarizers, and a temperature-controlled stage. Images were captured though a camera port utilizing a Nikon E950 digital camera.

AFM images of the crystalline forms of **2** were taken with a Dimension 3100 Nanoscope IV system (Veeco Metrology Group, Santa Barbara, CA). Tapping mode etched silicon probes with nominal force constants of 42 N/m and driving frequencies of 320 kHz were used for imaging. A single crystal of **2** was cast onto freshly cleaved mica from DMAC and 2 h was allowed for the solvent to evaporate prior to imaging. Images were recorded in tapping mode in air and displayed in both height and phase channels. AFM images of the single bilayer LB films of **2** on hydrophobized silicon were taken with a Multimode Nanoscope III system (Digital Instruments, Santa Barbara, CA) in contact mode in a solution of 0.1 M KCl. Oxide-sharpened silicon nitride probes with nominal force constant of 0.32 N/m were used, ozone cleaned for ca. 1 h prior to imaging. Images are displayed in both height and friction channels.

X-ray powder diffraction (XRD) measurements were conducted with a PANalytical X'Pert PRO MPD system with copper (Kα) radiation ($\lambda = 1.54$ Å) at 50 KV (40 mA target current). High-resolution scans were conducted along the goniometer axis ($\theta/2\theta$) at a step size of ca. 0.0167°. A fixed divergent slit of 1/4° was used in the incident beam optics, followed by an anti-scattering slit of 1/2°. X'Celerator, a RTMS (real time multiple strip) detector, was used in the diffracted beam optics, allowing faster data collection than conventional detectors without compromising resolution. Temperature-dependent XRD measurements were conducted with a capillary spinner sample holder and a capillary furnace with a high-temperature controller (Huber attachment 644 and HTC 9634, HUBER Diffraktionstechnik GmbH & Co. KG, Germany). The X-ray mirror was used in the incident beam optics with a beam divergence of 1/32° and the X'celerator, with a snout attachment, was used in the diffracted beam side. The X-ray generator was operated at 45 KV (40 mA target current) with continuous scans along 2θ at $\omega = 0°$ at step sizes of 0.0167°. Glass capillary tubes (Mark-Röhrchen, Aufnahmen) of 0.3 mm in diameter were used for most of the samples. Data analysis was done with *X'Pert Plus 1.0* from PANalytical.

Partial single-crystal structures were obtained from a stable polymorph of Pc **2** grown from dimethylacetamide (DMAC) solutions. Several crystals, each very thin green plates, of Pc **2** were mounted on a glass fiber in random orientations. The crystal giving the best diffraction had approximate dimensions of 0.48 × 0.11 × 0.02 mm. Examination of these crystals on a Bruker SMART 1000 CCD detector X-ray diffractometer at 170(2) K and a power setting of 50 KV, 40 mA, showed weak diffraction in each case. Diffraction data were obtained to $\theta = 16.5°$ (1.14 Å) for the strongest diffracting crystals. Data were collected on the SMART1000 system using graphite monochromatic Mo Kα radiation ($\lambda = 0.71073$ Å).

A total of 909 frames were collected at a single detector setting covering $-30° < 2\theta < +30°$, having a Φ scan width of 0.2° and an exposure time of 90 s. The frames were integrated using the Bruker SAINT software package's narrow frame algorithm. A total of 6820 reflections were integrated and retained, of which 3865 were unique ($\langle$redundancy$\rangle = 1.76$, $R_{int} = 25.37\%$, $R_{sig} = 48.45\%$). Of the unique reflections, 1158 (30.0%) were observed which were greater than $2\sigma(I)$. The final monoclinic cell parameters of $a =$ 23.911 (18) Å, $b = 5.724(3)$ Å, $c = 39.17(3)$ Å, $\alpha = 90°$, $\beta =$ 96.961(14)°, $\gamma = 90°$, volume = 4903(8) Å^3 are based on the refinement of the XYZ-centroids of 130 reflections with $I > 10\sigma(I)$ covering the range of $2.35° < \theta < 16.05°$. Given the poor redundancy, no correction for absorption was made. For $Z = 2$ and fw = 1907.933 the calculated density is 1.292 g cm^{-3}. Assignment of the space group from a poorly diffracting sample is difficult; systematic absences and intensity statistics indicate the space group to be *Pc* (No. 7).

The most promising partial structure solution was obtained using dual-space recycling followed by structure expansion using peak list optimization using ShelXM (part of the SHELXTL suite); a possible fragment corresponding to the expected copper−nitrogen core could be distinguished (Supporting Information). Expansion of this fragment using difference Fourier syntheses was unsuccessful. A Cu phthalocyanine core in the orientation obtained from the solution from XM was generated using a structure from the CSD. Constrained rigid body refinement of this fragment gave an *R*-factor of 45%; a random collection of atoms in a noncentrosymmetric space group would give an *R*-factor of about 60%. Unconstrained refinement of this phthalocyanine core fragment was not successful and it was not possible to locate any atoms from the side chains from Fourier maps. A reasonable packing structure of the molecules in this solution is described below.

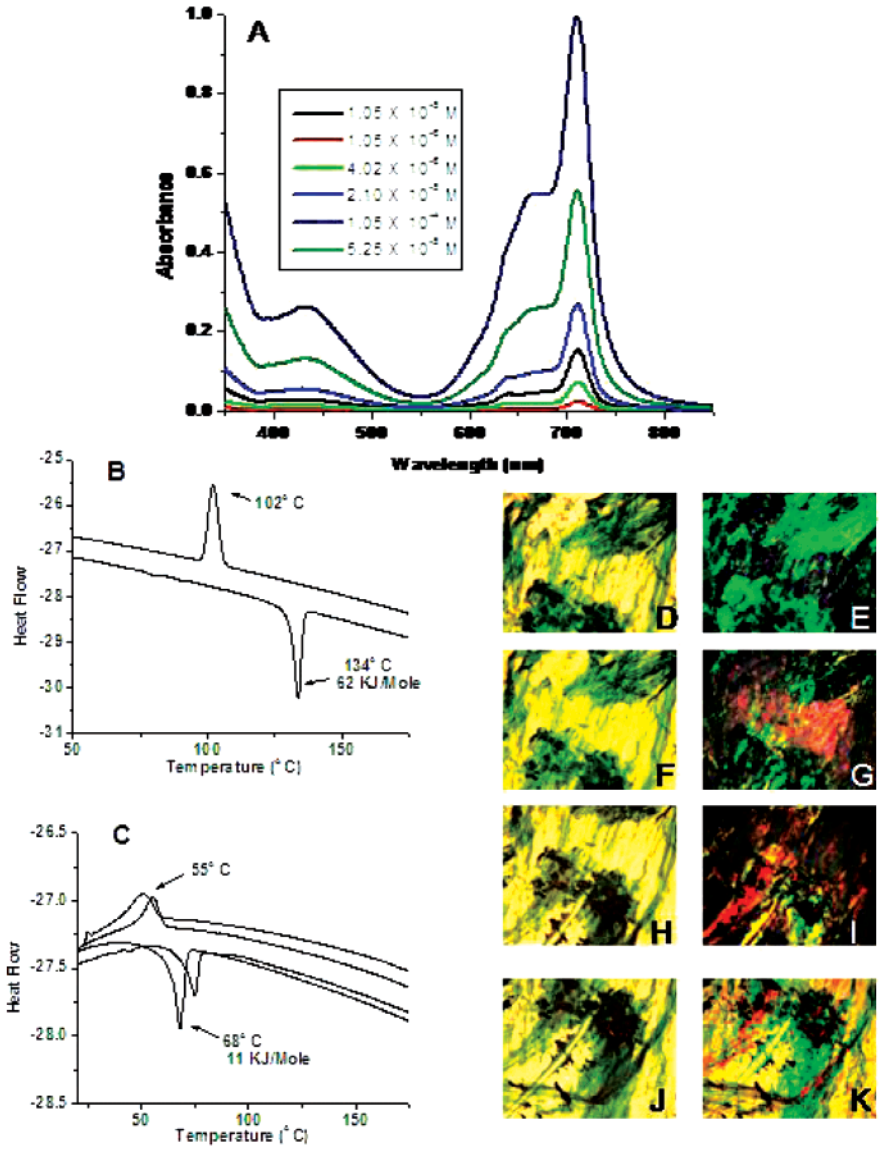

Figure 2. (A) Solution UV−Visible spectroscopy of solutions of **2** as a function of concentration (ca. 1×10^{-5} M to 5×10^{-5} M). The absorbances of the three most concentrated solutions were measured in a 0.1-cm cell; all other absorbances were measured in a 1-cm cell; all spectra are therefore normalized for ease of comparison. (B) DSC thermogram of a powder sample of **2**. (C) DSC thermogram of **1**. (D−K) Optical microscopy of overcompressed LB thin films (fibers) of Pc **2** captured on a glass substrate (left column, normal lighting; right column, with cross polarizers): (D/E) 28 °C; (F/G) 150 °C; (H/I) 315 °C; (J/K) cooled to 30 °C.

Results and Discussion

Synthesis of Pc 2. Figure 1 summarizes the synthetic scheme used to obtain gram quantities of Pc **2**. The thioether side chains for Pc **2** were prepared from commercially available benzyl-2-bromoethyl ether, **3**, (Aldrich) using a modification of a procedure by Svedhem and co-workers.[32] Potassium thioacetate was used to convert the alkyl bromide to thioacetic acid-S-(2-benzyloxyethyl) ester, **4**. The acetyl protecting group was next removed using either basic or acidic conditions to yield benzyloxyethanethiol, **5**, with yields ranging between 90 and 99%. The resulting thiol was reacted with 4,5-dichlorophthalonitrile to provide 4,5-bis-(2-benzyloxyethylsulfanyl)phthalonitrile, **6**, from which Pc **2** was prepared, following procedures developed by Tomoda and co-workers.[34] Both the copper-Pc, **2**, and demetalated version, **2′**, as well as the zinc version of this Pc have been prepared by this route. The overall yield from this synthesis for the CuPc version was typically 39%, and this route, which uses substantially gentler reaction conditions than previous sulfur-linked side chain Pc syntheses,[14] lends itself to scale-up to gram quantities of **2**. Comparable synthetic philosophies have been used to form Pcs with more complex side chains than those in **2**, including the addition of polymerizable groups, hydrogen-bonding groups, etc. to the side chain.[27]

Properties of Pc 2. As expected for sulfur-containing macrocycles,[11,12,14,35] the Q-band absorbance band for Pc **2** in chloroform (Figure 2A) is red-shifted ($\lambda_{max} = 711$ nm, $\epsilon_{711nm} = 1.3 \times 10^5$ $M^{-1}\cdot cm^{-1}$) versus the Q-band spectrum for Pc **1** ($\lambda_{max} = 678$ nm, $\epsilon_{678nm} = 1.5 \times 10^5$ $M^{-1}\cdot cm^{-1}$). As we have shown previously for solutions of **1**, The ratio of the aggregate absorbance peak to that for the monomeric species provides a way of estimating the solution aggregation constant (K_{agg}).[20,36] $K_{agg} = 420$ for **2** in chloroform solutions,

(35) Kobayashi, N.; Ogata, H.; Nonaka, N.; Luk'yanets, E. *Chem. Eur. J.* **2003**, *9*, 5123−5134.
(36) Tai, S.; Hayashi, N. *J. Chem. Soc., Perkin Trans 2* **1991**, 1275−1279.

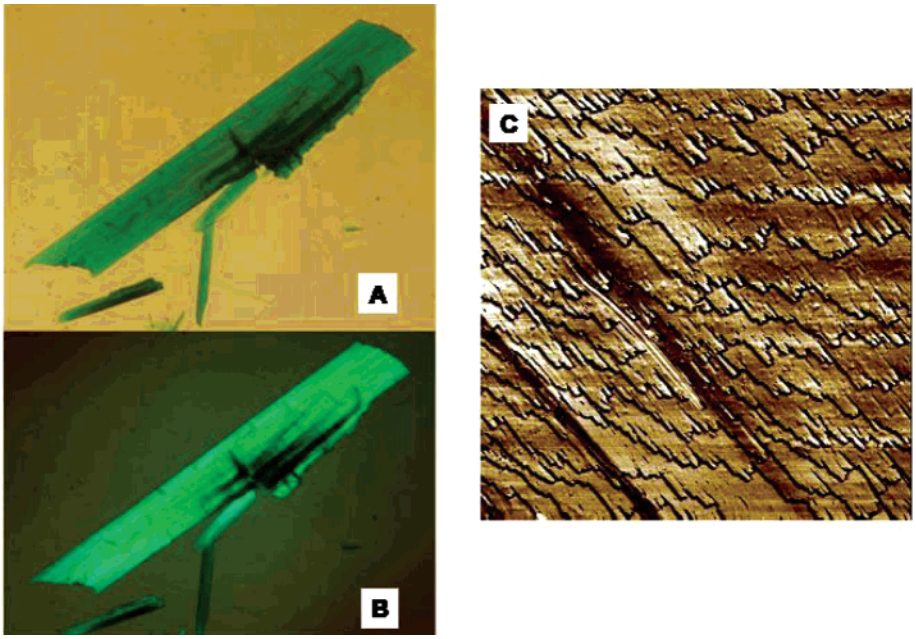

Figure 3. Left panel: Microscopy of an individual crystal of Pc **2** (ca. 50 micrometer length) after the anneal/cool cycle described in Figure 1: A, unpolarized light source; and B, with cross polarizers. (C) Tapping mode AFM image (5 μm × 5 μm) from the *c* face of a crystal like that shown at left, showing evidence for layered growth, with steps between the terrace regions of ca. 18−20 Å height, corresponding to one-half the *c*-axis dimension in the unit cell proposed for the single-crystal material (see text) (ref 31).

versus K_{agg} = 290 for solutions of **1**, suggesting that both molecules are weakly aggregating in chloroform solutions, versus other Pcs with electron-withdrawing substitutents linking the side chains, which has been shown to strengthen arene−arene interactions,[20,36] but that the addition of chalcogen linkers of the benzyl terminated side chains does enhance the interaction over the alkoxy linkers.

First oxidation potentials were determined in methylene chloride (0.1 M $LiClO_4$) for both Pc **2** (+0.145 V vs Fc/Fc^+) and Pc **1** (+0.200 V vs Fc/Fc^+).[27] The increased solution aggregation constant for **2** suggests somewhat stronger Pc−Pc interactions, even in solvents where the molecule demonstrates good solubility. The less positive first oxidation potential suggests that the macrocycle is more electron-rich, and therefore slightly more reactive toward oxidation by both intentionally added, and adventitious, dopants. Additional characterization of first ionization potentials in thin films, and the implications for the positions of these energy levels in OPV devices will be described in forthcoming reports.

Differential scanning calorimetry (DSC) of bulk powders of **2** (Figure 2B) shows a sharp K→LC phase transition at ca. 134 °C with an endotherm/exotherm hysteresis of 32°, attributed to a super cooling of the side chain regions of the material.[4−7] The increased steric bulk and interaction of the thioether groups is expected to lower the mobility of the side chains as they cool, after reaching the LC mesophase temperature. The LC mesophase of **2** is stable to 299 °C in air, no clearing point is seen prior to decomposition. In contrast, a K→D_h transition is seen for **1** (and related Pcs) at lower temperatures (68 °C), with smaller hysteresis (13°) (Figure 2C). The energy associated with the K→LC transition is 62 kJ/mol for **2** and 11 kJ/mol for **1**. If the primary energy difference is due to chalcogen−chalcogen interactions, each thioether group in **2** adds ca. 6.4 kJ/mol interaction energy (literature values of 2−9 kJ/mol have been reported for other chalcogen−chalcogen interactions).[30] As expected for discotic mesophase liquid crystalline materials, fibers of **2** harvested from overcompressed films on an LB trough,[23] viewed with polarized optical microscopy (Figure 2, right panel, D/E−J/K), show increased birefringence at the K→LC transition, and loss of this birefringence at higher temperatures. Small single crystals of **2** were isolated from DMAC solutions, and the birefringence seen in these crystals (Figure 3A vs B) is enhanced by the same heating/cooling cycle.[27]

X-ray Diffraction and AFM Studies of Polycrystalline and Single-Crystal Polymorphs, and LB Films, of Pc 2. X-ray diffraction of powders of Pc **2**, harvested from chloroform solutions, and single crystals of Pc **2**, grown from DMAC solutions, suggest that this molecule can exist in at least two closely related polymorphs. XRD of powders of **2**, harvested from chloroform solutions (Figure 4a), gave a fully indexed pattern, with large Bragg peaks from the ⟨100⟩, ⟨001⟩, and ⟨10$\bar{1}$⟩ planes. Diffraction from the ⟨010⟩ planes was systematically absent. Monoclinic unit cell parameters were estimated from this diffraction data: a = 22.81(1) Å, b = 9.780(5) Å, c = 19.314(6) Å, α = 90°, β = 106.918(14)°, γ = 90°, V = 4472 Å^3, two molecules per unit cell. The temperature-dependent XRD data (Figure 4b), show that near ca. 133 °C the major diffraction peaks are joined by two new peaks (2θ = 3.9° and 4.2°), which dominate as the temperatures rise into the LC regime, consistent with the formation of an oblique (distorted rectangular, Col_{rd}) phase.[10,37] Upon cooling to room temperature, the diffraction pattern of the original crystalline phase is recovered. This diffraction data is in sharp contrast to XRD of powders and fibers of Pc **1**, where the room-temperature phase is much less ordered, and the LC-mesophase gives a diffraction pattern

(37) *Handbook of Liquid Crystals*; Demus, D., Goodby, J., Gray, G. W., Spiess, H.-W., Eds.; Wiley-VCH: New York, 1998; Vol. 1: Fundamentals.

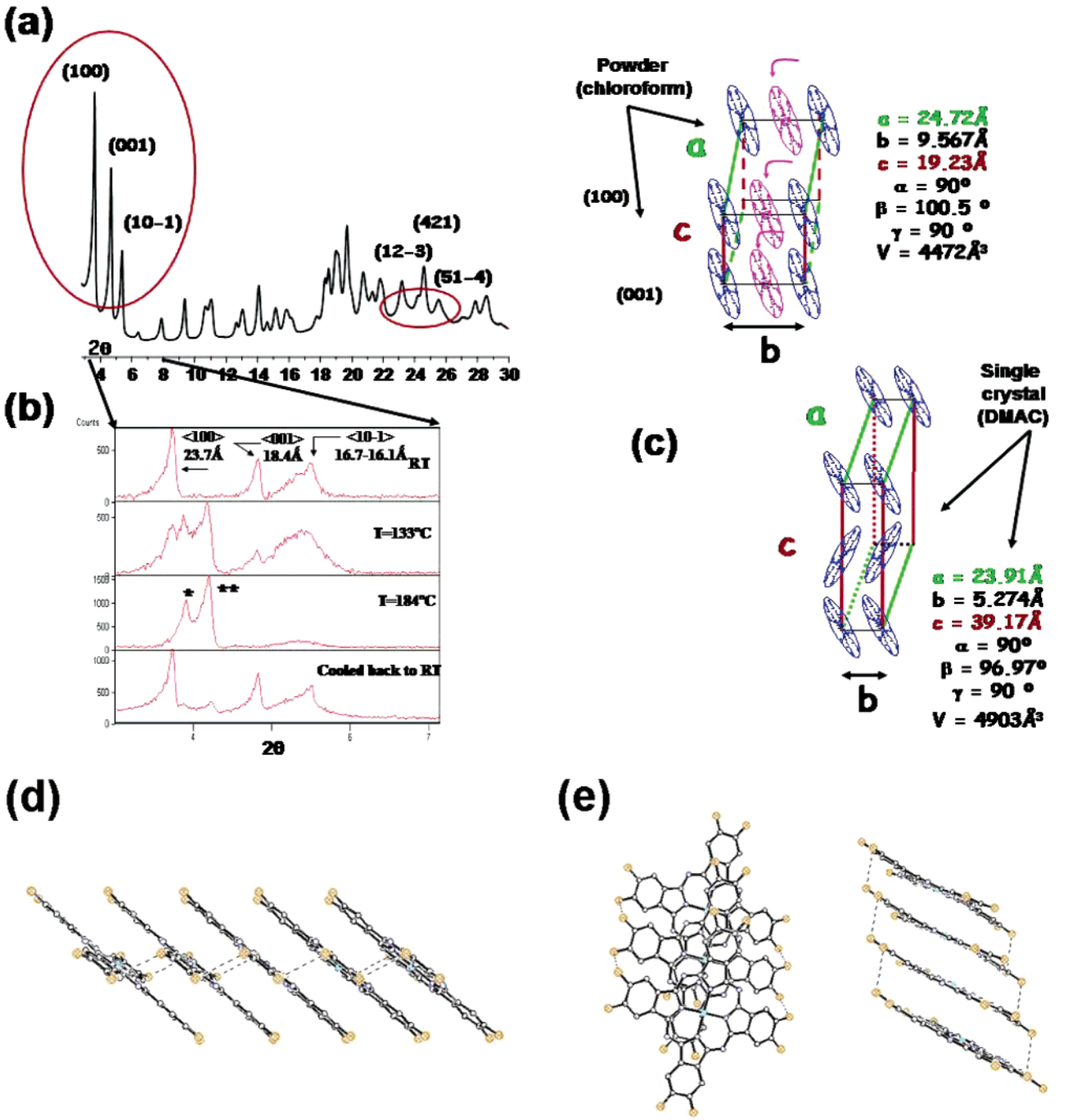

Figure 4. (a) Room-temperature powder X-ray diffraction data for **2**, with three well-defined Bragg peaks at 3.60°, 4.65°, and 5.35° in 2θ from the ⟨100⟩, ⟨001⟩, and ⟨10-1⟩ planes, respectively. (b) Expansion of the low angle region in (a), showing the disappearance of the major reflections in the crystalline phase as the K→LC transition is reached (T = 133 °C), the formation of new reflections (*) and (**) (T = 184°) suggesting formation of an oblique (distorted rectangular) columnar phase (Col_{rd}), followed by the return to the original diffraction pattern upon cooling to room temperature. An additional peak is seen near the ⟨10-1⟩ reflection arising from the hood needed to maintain uniform temperature control of the capillary during heating. (c) The unit cells proposed from both the powder XRD data (upper), and the single-crystal data (lower), arising from different polymorphs of **2**. (d) Proposed packing of the molecules into columns parallel to the *b* axis in the single-crystal structure. The dashed lines indicate S···S contacts of 3.52 Å. (e) Proposed relative orientation of molecules in two adjacent columns (along the *c* axis) in the single crystal.

typical of a hexagonal columnar phase, with a single Pc−Pc stacking distance and a single Pc−Pc column distance.[20,21,29,31]

Small single crystals of **2** grown from DMAC solutions have been obtained with sufficient size to provide a partial X-ray structure; the largest single crystals obtained are thin plates (0.48 × 0.11 × 0.02 mm maximum size), providing sufficient detail in the diffraction data to estimate the position of the Pc rings within the structure, but not enough detail to identify the exact location and orientation of the side chains.[13] Monoclinic unit cell parameters are a = 23.911 (18) Å, b = 5.224(3) Å, c = 39.17(3) Å ($c \approx \sqrt{3}a$); α = 90°, β = 96.971-(14)°, γ = 90°, volume = 4903(8) Å^3 (see Supporting Information).

The primary differences in these two polymorphs are revealed in comparison of the *b*-axis and *c*-axis unit cell lengths (schematics shown in Figure 4c). The *b*-axis length from the powder diffraction data in Figure 4a and b is ca.

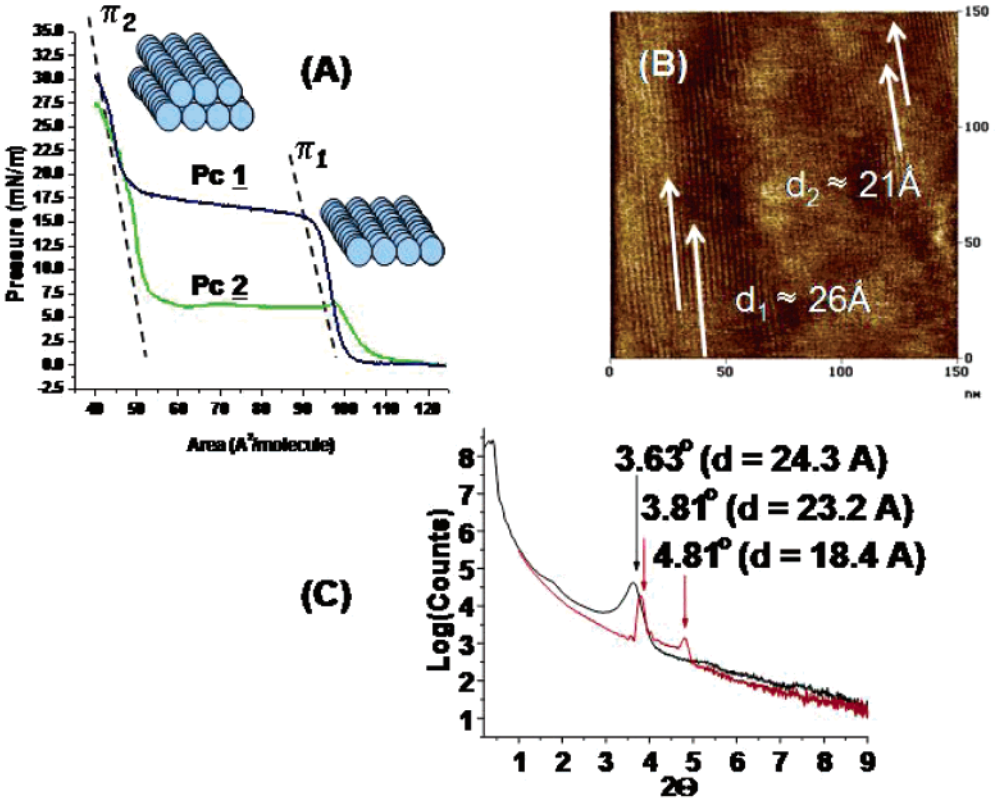

Figure 5. (A) Pressure−area isotherms for Pc **1** and Pc **2**: the first transition at π_1 represents formation of a stable monolayer of parallel rodlike aggregates; the second transition at π_2 represents formation of a stable bilayer of similar rods. Films are typically horizontally transferred to various substrates at the second transition. Stable fibers of either **1** or **2** are formed at pressures beyond π_2 (refs 11−13, 21). (B) Contact mode AFM image, in aqueous solution, of a single bilayer LB film of **2** transferred to hydrophobized Si(100), annealed in a vacuum (180 °C, 4 h). Two different column−column periodicities of ca. 21 and 26 Å are seen. (C) X-ray reflectivity data for a 10-bilayer, horizontally transferred LB film of **2** on hydrophobized Si(100) (black curve shows the unannealed film). The first Bragg peak is at 3.63° which corresponds to a *d* spacing of 24.3 Å. After annealing at 180 °C (red curve), two Bragg peaks are observed for this same thin film: the first peak is at 3.81° (*d* spacing of 23.2 Å), and a less intense peak at 4.8° (*d* spacing of 18.4 Å). These spacings are close to the dimensions of the *a* and *c* axes of the unit cell proposed above from the XRD data, suggesting that annealed multilayer LB ilms can adopt either the ⟨100⟩ or the ⟨001⟩ planes of the powder unit cell in Figure 4.

2× that observed from the single crystal diffraction data, and the *c*-axis length in the single crystal unit cell is ca. 2× the value seen in the powder diffraction data, suggesting a simple interconversion between these two structures. The single crystal data are consistent with there being only one Pc orientation along the *b*-axis (Figure 4d); within one column the Cu atoms in adjacent Pcs appear to be 5.3 Å apart (the *b* unit cell length from the single-crystal data), however, the tilt of the Pcs within each column provides for sulfur atoms on adjacent molecules to be as close as ca. 3.5 Å (ca. twice the van der Waals radius of sulfur), consistent with strong S−S interactions.[30,31,37] The parallel columns in the single crystal are related by crystallographic symmetry: along the *a* axis the columns are related by translational symmetry; along the *c* axis the columns are related by a *c* glide (Figure 4e); the orientation of molecules in adjacent columns appears to alternate by 98°, therefore a herringbone packing of the Pc columns along the *c* axis is observed. This proposed unit cell for **2** provides for layered crystalline growth, which is consistently confirmed in AFM images (Figure 3c) of one face of the single crystal (the ⟨001⟩ plane). Step heights between the terraces are ca. 18−20 Å (ca. $^1/_2$ the *c*-axis dimension of the unit cell), which demonstrates layered growth in the bulk crystals, and as will be discussed elsewhere, represents one of the dominant growth faces seen in annealed spin-cast thin films of this material.[31]

The powder diffraction data suggest alternating Pc orientations along the *b* axis: each Pc along this axis is rotated in-plane by ca. 45° with respect to its nearest neighbor, which provides for the extinction of the ⟨010⟩ reflection in the XRD data.[31] This rotation provides for a means of close packing of adjacent Pc disks, accommodating the increased (out-of-plane) size of sulfur links, versus oxygen links, to the side chains. This kind of helical twist has been observed in other discotic mesophase materials, where sulfur is incorporated into the disk, as a side-chain linker.[3] Although the schematic views in Figure 4c suggest side chains that are in the plane of the Pc ring, their exact position is unknown, and is likely to be substantially out-of-plane to accommodate the most efficient packing of adjacent disks. During the K→LC transition, the powder diffraction data suggest that the packing of Pc columns changes only slightly, and the loss of long-range order along the column axis at the LC phase is mainly due to disordering of these side chains. This is in contrast to Pc **1**, where the K→LC transition is accompanied by a clear change of the tilt angle of the Pc disks to a pure hexagonal mesophase; the full details of these transitions, comparing both sulfur-linked and oxygen-linked derivatives of **1** and **2**, are reported elsewhere.[31]

Both Pcs **1** and **2** form ordered LB films, with parallel columnar Pc aggregates.[9,21,25,28,33] Comparable monolayer→bilayer pressure−area transitions are seen for both molecules;

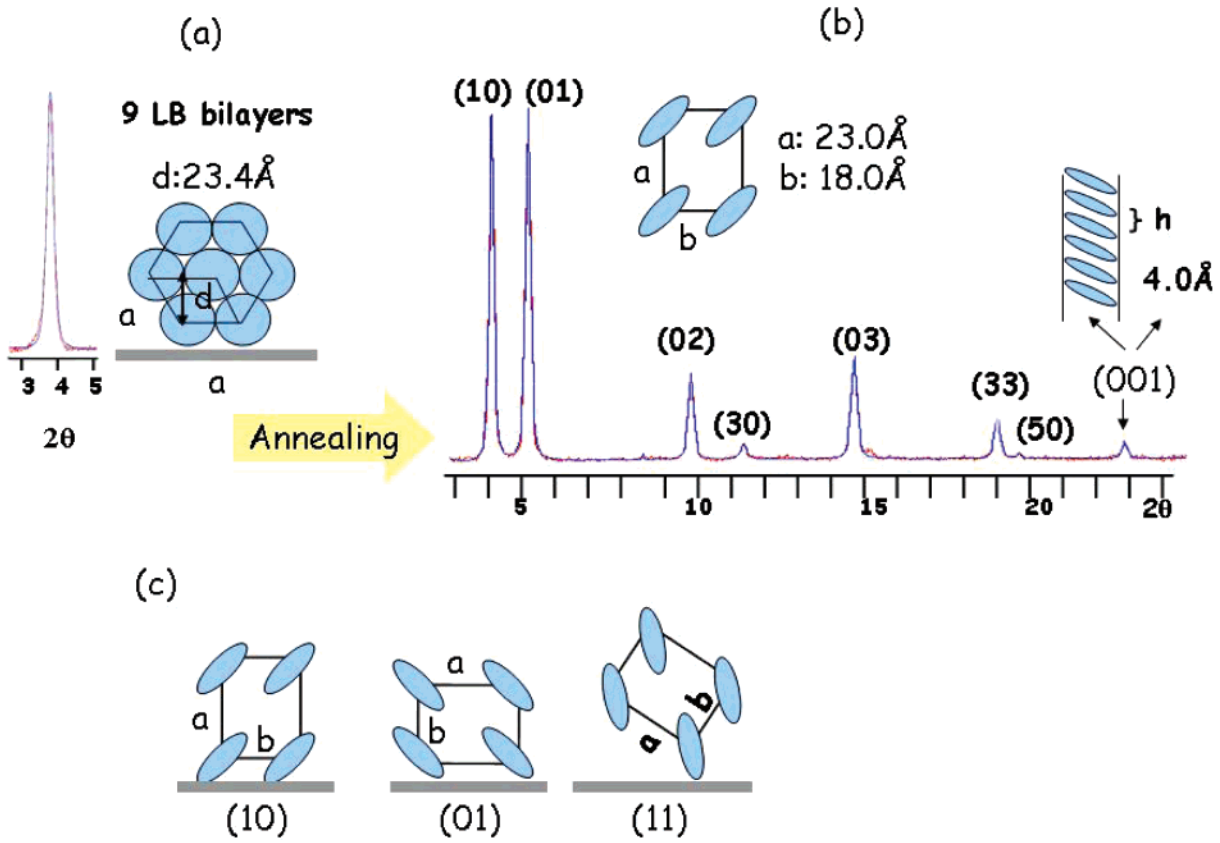

Figure 6. (a) X-ray diffraction (red, data; blue, background-corrected, fitted data) of an as-deposited 9-bilayer LB film of Pc **2**: a single 2D hexagonal phase dominates the as-deposited film with a single Bragg peak at 2θ = ca. 3.9° indicating an intercolumn spacing of 23.4 Å. (b) The XRD data for the same film after annealing/cooling (K→LC→K). The diffraction pattern of the annealed film can be indexed into a 2D rectangular phase with dimensions of a = 23.0 Å and b = 18.0 Å, very close to the a and c dimensions of the unit cell determined from powder XRD data (Figure 5). Three different faces of the 2D lattice are indicated in these data. The Bragg peaks at 2θ = 3.86° and 4.93° represent the ⟨10⟩ and ⟨01⟩ faces respectively, as seen in the AFM/XRR data in Figure 5. The Bragg peak at 18.6° represents the (33) reflection for the (11) face, and is a minor component in the film structure, and was not seen in the AFM data of Figure 5. The schematics in (c) show the possible geometries, ⟨10⟩, ⟨01⟩, and ⟨11⟩ planes, adopted by the annealed LB films. The reflection at 2θ = ca. 22.4° (lattice spacing of ca. 4 Å) cannot be indexed as part of the 2D lattice, and is most likely due to the intracolumn Pc−Pc spacing when a small fraction of the columns of Pc **2** are tilted upright with respect to the substrate, providing for an ⟨001⟩ plane of a 3-dimensional lattice.

however, the pressures associated with these transitions are lowered in **2** versus those seen for **1**,[27,31] i.e., the pressure needed to complete a close-packed monolayer array, and to begin the formation of the close-packed bilayer array, is lowered for Pc **2** vs Pc **1**. As previously discussed for Pc **1**,[21,25,29,33] these films can be reversibly compressed and expanded if the compression barriers are stopped at the first transition (π_1). Compression to the point where a stable bilayer can be formed (π_2) does not allow for a reversible expansion of the film, i.e., formation of the close packed arrays of parallel columns produces sufficient column−column interactions as to leave the film in a semirigid state, which can be cut into sections and horizontally transferred to appropriately modified substrates.[29,33]

AFM images of annealed bilayer films of **2** transferred to hydrophobized Si(100)/native oxide substrates (Figure 5A) showed two different column−column periodicities after vacuum annealing above the K→LC transition temperature and back to room temperature, at ca. 21 Å and ca. 26 Å. X-ray reflectivity data for multilayer films (Figure 5C) shows one broad peak (d = 24.3 Å) for the as-deposited film, and one major (d = 23.2 Å) and one minor (d = 18.4 Å) peak after this annealing/cooling cycle. These spacings along the surface normal from XRR are close to those observed for the a and c axes of the powder diffraction unit cell (Figure 4).

Figure 6 provides additional insight as to the nature of the packing of Pc **2** in as-deposited and annealed LB films. Figure 6a shows a portion of the XRD data for an as-deposited 9 bilayer film of Pc **2**: these data showed only one major Bragg peak at 2θ = 3.86°, consistent with a hexagonal close packed array of Pc columns, with a d spacing of 23.4 Å. After annealing this multilayer film (K→LC→K) the XRD data of Figure 6b were observed which showed a pattern of diffraction peaks which could be fully indexed for a 2D rectangular phase with dimensions of a = 23.0 Å and b = 18.0 Å, very close to the a and c axis dimensions of the unit cell determined from powder XRD data (Figure 5). The Bragg peaks at 2θ = 3.86° and 4.93° represent the ⟨10⟩ and ⟨01⟩ faces of this 2D lattice, respectively, as seen in the AFM/XRR data in Figure 5. The Bragg peak at 18.6° appears to represent a ⟨33⟩ reflection for the ⟨11⟩ face of this lattice, and is a minor component in the film structure, and was not seen in the AFM data of Figure 5. The schematics in Figure 6c show the possible geometries of the ⟨10⟩ ⟨01⟩ and ⟨11⟩ planes which could be adopted by the annealed LB films. The reflection at 2θ = ca. 22.4° (lattice spacing of ca. 4 Å) could not be indexed and is most likely

due to intracolumn ordering within regions in the LB film where molecules of Pc **2** are arranged as vertically aligned columns. The ordering along the third dimension (the column axis) is represented by the far right schematic in Figure 6b.

The ordering of bilayer and multilayer films of **2** into this 2D lattice is in sharp contrast to LB films of **1**, which generally show only one packing architecture after annealing, consistent with their greater tendency to adopt a hexagonal close-packed arrangement of parallel Pc columns.[21,23,33] Significant optical and electrical anisotropies occur with annealed films of **1**. LB-deposited, spin-cast and drop-cast and annealed films of **2**, however, show a much greater tendency to form up to three different column packing architectures, and are therefore expected to show a much greater heterogeneity in their optical and electrical properties, probed on submicron length scales.

Conclusions

The change of 2-benzyloxyethoxy side chains in Pc **1** to 2-benzyloxyethylsulfanyl side chains in **2** enhances their ability to self-organize, through S−S interactions, and produces an unusual crystalline phase in powders which can reversibly form an oblique (distorted rectangular) liquid crystalline phase (K→Col_{rd}→K). The LB films of these materials, which are the type of Pc film used as the active channel region in OFETs,[28] clearly show two different column−column spacings upon annealing, closely related to those seen in the crystalline powders. Current studies are focusing on characterization of the electrical properties of thin crystals of **2** on the nanometer length scale, and the application of spin-cast and drop-cast films of these Pcs, and related thioether phenyl-terminated octa-substituted Pcs, on modified substrate, in organic photovoltaic devices and organic field-effect transistors.[38]

Acknowledgment. We gratefully acknowledge support of this research by the National Science Foundation (NRA CHE-0211900; DFO/NRA DMR-0087587), the Office of Naval Research; the DOE-NREL "Photovoltaics Beyond the Horizon" program, and the NSF-Center for Materials and Devices for Information Technology DMR-0120967. W.X. acknowledges support of the Pfizer Corporation for a graduate fellowship 2004/2005. We also gratefully acknowledge the assistance of Jim Cain in the ^{1}H-NMR studies of the Pc **2**.

Supporting Information Available: Details for characterization of **2** by mass spectrometry and NMR (pdf). This material is available free of charge via the Internet at http://pubs.acs.org.

CM0483745

(38) Yoo, S.-Y.; Domercq, B.; Donley, C.; Carter, C.; Xia, W.; Minch, B. A.; O'Brien, D. F.; Armstrong, N. R.; Kippelen, B. Organic photovoltaic cells contining discotic liquid crystalline phthalocyanines. In *Organic Photovoltaics IV*; Kafafi, Z. H., Lane, P. A., Eds.; SPIE - International Society for Optical Engineering: Bellingham, WA, 2004; p 71.